The Open Biotechnology Journal
DOI: 10.2174/0118740707426277251205182540, 2026, 20, e18740707426277
ISSN: 1874-0707
1

RESEARCH ARTICLE **OPEN ACCESS**

Antimicrobial Efficacy of Multiwalled Carbon Nanotube Suspensions Against Multidrug-Resistant *Stenotrophomonas maltophilia*: A Comprehensive *In Vitro* Analysis

Abeer Abdulridha Abass[1], Israa Abdul Ameer Al-Kraety[2], Sddiq Ghani Al-Muhanna[2], Wasna'a Mohamed Abdulridha[3], Abtesam Imhmmed Aljdaimi[4], Akrem Jalal-Karim[2] and Salah M. Ibrahim[5,*]

[1]*Department of Basic Science, Faculty of Dentistry, Kufa University, Najaf, Iraq*
[2]*Department of Medical Laboratory, College of Health and Medical Technology, University of Alkafeel, Najaf, Iraq*
[3]*Department of Physical College of Science, University of Kufa, Najaf, Iraq*
[4]*Department of Conservative Dentistry, Faculty of Dentistry, Alasmarya Islamic University, Zliten, Libya*
[5]*Department of Oral Surgery, College of Dentistry, Kufa University, Iraq*

Abstract:

Background: The emergence of multidrug-resistant (MDR) *Stenotrophomonas maltophilia* poses significant therapeutic challenges in clinical settings. This opportunistic gram-negative bacterium exhibits extensive antibiotic resistance mechanisms and forms biofilms on medical devices. Multiwalled carbon nanotubes (MWCNTs) have emerged as promising antimicrobial agents due to their unique physicochemical properties and multiple mechanisms of action.

Materials and Methods: Thirty clinical samples were collected from Kufa University Medical Center (November 2023-March 2024), yielding 20 confirmed *S. maltophilia* isolates through VITEK-2 identification. MWCNTs were synthesized *via* thermal decomposition and characterized using AFM, SEM, XRD, and FTIR. Antimicrobial activity was evaluated using well diffusion and broth microdilution methods at 25, 50, 75, and 100 µg/mL concentrations. Biofilm assays were performed using crystal violet staining. Results were compared with six conventional antibiotics.

Results: MWCNT characterization revealed 82.74 ± 5.2 nm grain size with armchair geometry. MWCNT suspensions demonstrated concentration-dependent antimicrobial activity, with 100 µg/mL producing 22.7 ± 1.58 mm inhibition zones, exceeding most antibiotics except ciprofloxacin (25.1± 4.98 mm). MIC values were 18.4 ± 10.01 µg/mL (MIC_{50} = 12.5 µg/mL). Biofilm formation was significantly reduced, with 100% MWCNT (The 100 µg/mL suspension) achieving 97.3% inhibition. All isolates exhibited high antibiotic resistance (75-95%).

Discussion: The superior antimicrobial activity of MWCNTs demonstrates their potential as alternative therapeutic agents for MDR *S. maltophilia* infections. Multiple mechanisms, including physical membrane disruption, reactive oxygen species generation, and metabolic interference, explain effectiveness against resistant isolates. The exceptional biofilm inhibition addresses critical clinical challenges, as *S. maltophilia* biofilms are difficult to eradicate with standard antibiotics. Clinically achievable MIC values support therapeutic feasibility.

Conclusion: MWCNT suspensions possess potent antimicrobial activity against MDR *S. maltophilia* with superior biofilm inhibition properties. The ability to overcome resistance mechanisms suggests MWCNTs represent promising alternatives for treating *S. maltophilia* infections, warranting further safety evaluation and clinical development.

Keywords: Antimicrobial activity, Biofilm inhibition, Minimum inhibitory concentration, Multidrug resistance, Multiwalled carbon nanotubes, Nanotechnology, Opportunistic pathogen, *Stenotrophomonas maltophilia*.

*Address correspondence to this author at the Department of Oral Surgery, College of Dentistry, Kufa University, Iraq; E-mail: salahm.abrahem@uokufa.edu.iq

Cite as: Abass A, Al-Kraety I, Al-Muhanna S, Abdulridha W, Aljdaimi A, Jalal-Karim A, Ibrahim S. Antimicrobial Efficacy of Multiwalled Carbon Nanotube Suspensions Against Multidrug-Resistant *Stenotrophomonas maltophilia*: A Comprehensive *In Vitro* Analysis. Open Biotechnol J, 2026; 20: e18740707426277.
http://dx.doi.org/10.2174/0118740707426277251205182540

Received: June 29, 2025
Revised: September 22, 2025
Accepted: October 06, 2025
Published: March 02, 2026

1. INTRODUCTION

The global healthcare landscape faces an unprecedented challenge from the emergence and spread of multidrug-resistant (MDR) bacterial pathogens, which threaten to reverse decades of progress in infectious disease management [1]. Among these concerning pathogens, *Stenotrophomonas maltophilia* has become a particularly problematic gram-negative, opportunistic bacterium that presents significant therapeutic difficulties in clinical settings [2]. This non-fermentative, aerobic, motile bacterium with polar flagella has developed sophisticated resistance mechanisms that make conventional antibiotic treatments increasingly ineffective, especially in immunocompromised patients [3]. *S. maltophilia* exhibits a complex array of virulence factors that enhance its pathogenic potential and clinical importance. The bacterium possesses cell-associated virulence structures, including lipopolysaccharides, pili, non-pilus adhesins, and flagella, which enable it to adhere to both living and non-living surfaces [4]. Additionally, *S. maltophilia* produces numerous extracellular virulence factors, such as proteases, lipases, esterases, deoxyribonuclease, ribonuclease, hyaluronidase, hemolysins, cytotoxins, and siderophores, which facilitate tissue invasion and immune system evasion [5]. Recent research has shown that clinical isolates of *S. maltophilia* exhibit greater virulence traits compared to environmental strains, particularly their ability to form biofilms and display twitching motility at human body temperature (37°C), a critical adaptation for pathogenicity [6].

The intrinsic resistance profile of *S. maltophilia* encompasses a broad spectrum of antibiotics, including β-lactams, aminoglycosides, carbapenems, and macrolides, primarily due to chromosomally encoded resistance mechanisms [7]. Furthermore, the bacterium can acquire additional resistance through horizontal gene transfer and mutations, creating an ever-evolving challenge for antimicrobial therapy [8]. This multifaceted resistance pattern has positioned *S. maltophilia* as one of the leading MDR organisms in hospital settings, where it causes nosocomial infections, including bacteremia, endocarditis, pneumonia, meningitis, ocular diseases, urinary tract infections, enteritis, and skin and soft tissue infections [9].

The clinical management of *S. maltophilia* infections is further complicated by the bacterium's remarkable ability to form biofilms on medical devices, including implants and catheters, which significantly increases the risk of device-associated infections and treatment failure [10]. Biofilm formation not only protects against host immune responses but also creates a barrier that reduces antibiotic penetration and efficacy, necessitating higher drug concentrations that may be associated with increased toxicity [11]. Recent studies have demonstrated that the ability to express these virulence traits at human body temperature is a distinguishing feature of pathogenic *S. maltophilia* strains, highlighting the importance of temperature adaptation in clinical pathogenesis [12].

In response to the growing threat of antimicrobial resistance, the scientific community has increasingly focused on developing novel therapeutic strategies that can circumvent traditional mechanisms of resistance. Nanotechnology has emerged as a particularly promising field, offering innovative approaches to combat MDR pathogens through unique mechanisms of action that differ fundamentally from conventional antibiotics [13]. Among various nanomaterials, carbon nanotubes (CNTs) have garnered significant attention due to their exceptional physicochemical properties and demonstrated antimicrobial efficacy against a wide range of bacterial pathogens [14].

Carbon nanotubes, particularly multiwalled carbon nanotubes (MWCNTs), represent a class of cylindrical nanostructures composed of graphite sheets rolled into seamless tubes with remarkable mechanical, electrical, and thermal properties [15]. These nanomaterials possess unique characteristics, including ultralight weight, high tensile strength, metallic electronic properties, and exceptional chemical and thermal stability, making them suitable for a diverse range of biomedical applications [16]. Recent comprehensive reviews have identified multiple mechanisms by which MWCNTs exert their antimicrobial effects, including physical membrane disruption through direct contact, generation of reactive oxygen species (ROS) leading to oxidative stress, and interference with essential metabolic pathways [17].

The antimicrobial activity of MWCNTs arises from several interconnected mechanisms that work together to kill bacteria. Physical damage to the membrane is a primary mechanism, where MWCNTs can physically pierce bacterial outer membranes, causing irreversible structural damage and cell lysis [18]. This direct contact-based process is especially effective because it bypasses traditional resistance pathways that bacteria have developed against

conventional antibiotics. Additionally, MWCNTs promote the formation of reactive oxygen species, including hydroxyl radicals and superoxide anions, which cause oxidative stress in bacterial cells and ultimately lead to cell death [19].

Recent research has shown that the antimicrobial efficacy of MWCNTs depends on various factors, including their diameter, length, surface functionalization, concentration, and specific bacterial target [20]. MWCNTs with smaller diameters generally show increased toxicity against different bacterial species, with effects that are strain-dependent and related to higher surface area-to-volume ratios [21]. The surface charge of MWCNTs also significantly impacts their antimicrobial activity, with both positively and negatively charged nanotubes demonstrating bactericidal effects through different mechanisms involving membrane interaction and cellular uptake [22].

The development of MWCNT-based antimicrobial strategies represents a paradigm shift in addressing antibiotic resistance, as these nanomaterials operate through multiple simultaneous mechanisms that are difficult for bacteria to circumvent through traditional resistance pathways [23]. Unlike conventional antibiotics that typically target specific cellular processes, MWCNTs exert their effects through physical disruption, chemical interaction, and oxidative stress induction, creating a multi-pronged attack that overwhelms bacterial defense mechanisms [24].

Furthermore, recent studies have shown that MWCNTs can improve the effectiveness of traditional antibiotics when used together, potentially overcoming resistance mechanisms like efflux pumps and enzymatic degradation [25]. This synergistic approach offers the chance to restore the power of existing antibiotics while also providing new antimicrobial activity through nanotechnology-based methods [26].

The biofilm-disrupting properties of MWCNTs represent another significant advantage in treating *S. maltophilia* infections, as these nanomaterials can penetrate biofilm matrices and disrupt the protective environment that shields bacteria from antimicrobial agents [27]. This capability is particularly relevant for *S. maltophilia*, given its propensity for biofilm formation on medical devices and its role in device-associated infections [28].

Despite the promising antimicrobial properties of MWCNTs, several challenges remain in translating these findings into clinical applications. Safety considerations, including potential cytotoxicity and environmental impact, require careful evaluation through comprehensive toxicological studies [29]. Additionally, optimization of synthesis methods, surface functionalization strategies, and delivery systems is essential for maximizing therapeutic efficacy while minimizing adverse effects [30].

The current study fills a critical gap in the literature by specifically examining the antimicrobial effectiveness of MWCNT suspensions against clinical isolates of *S. maltophilia*, a pathogen of growing clinical concern due to its inherent and acquired resistance mechanisms. By comparing the antimicrobial activity of MWCNTs with traditional antibiotics and evaluating their ability to disrupt biofilms, this research adds to the expanding evidence supporting the development of nanotechnology-based treatments for combating MDR bacterial infections.

2. MATERIALS AND METHODS

2.1. Ethical Approval and Compliance

This study was conducted in accordance with the Declaration of Helsinki and approved by the Institutional Review Board of Kufa University (Ethics Committee Reference Number: KU-IRB-2023-089). Written informed consent was obtained from all patients or their legal guardians before sample collection. All procedures involving human subjects were performed in compliance with relevant guidelines and regulations. Patient confidentiality was maintained throughout the study, and all samples were de-identified before analysis.

2.2. Sample Size Determination

The sample size was calculated based on the expected prevalence of *S. maltophilia* in clinical specimens (15-25%) and required statistical power for antimicrobial testing. Using the formula $n = Z^2p(1-p)/d^2$ with $Z = 1.96$, $p = 0.20$, and $d = 0.15$, a minimum of 28 specimens was required. The sample size was increased to 30 specimens to account for potential losses, providing adequate power ($\beta = 0.80$, $\alpha = 0.05$) to detect significant differences between MWCNT suspensions and conventional antibiotics.

2.3. Study Design and Sample Collection

A prospective cross-sectional study was conducted from November 2023 to March 2024 at the University of Kufa Medical Center and its affiliated healthcare facilities in Najaf, Iraq. Clinical samples were gathered from patients with infectious conditions, including urinary tract infections, gastroenteritis, and otitis externa. A total of 30 specimens were collected, consisting of 15 urine samples (50%), 10 stool samples (33.3%), and 5 ear swab samples (16.7%). All samples were collected using sterile techniques and transported to the laboratory within 2 hours of collection in suitable transport media.

The inclusion criteria for the study required patients to exhibit clinical signs and symptoms of bacterial infection, be at least 18 years old, have not received antibiotic treatment within 48 hours before sample collection, and provide written informed consent. The exclusion criteria removed patients with incomplete clinical data, samples with insufficient volume for analysis, specimens contaminated with mixed bacterial growth, patients who withdrew consent, and individuals with immunocompromising conditions or undergoing immunosuppressive therapy.

The comprehensive methodology adopted for evaluating the antibacterial effects of multiwalled carbon nanotubes is illustrated in Fig. (**1**), which demonstrates the systematic approach employed in this investigation.

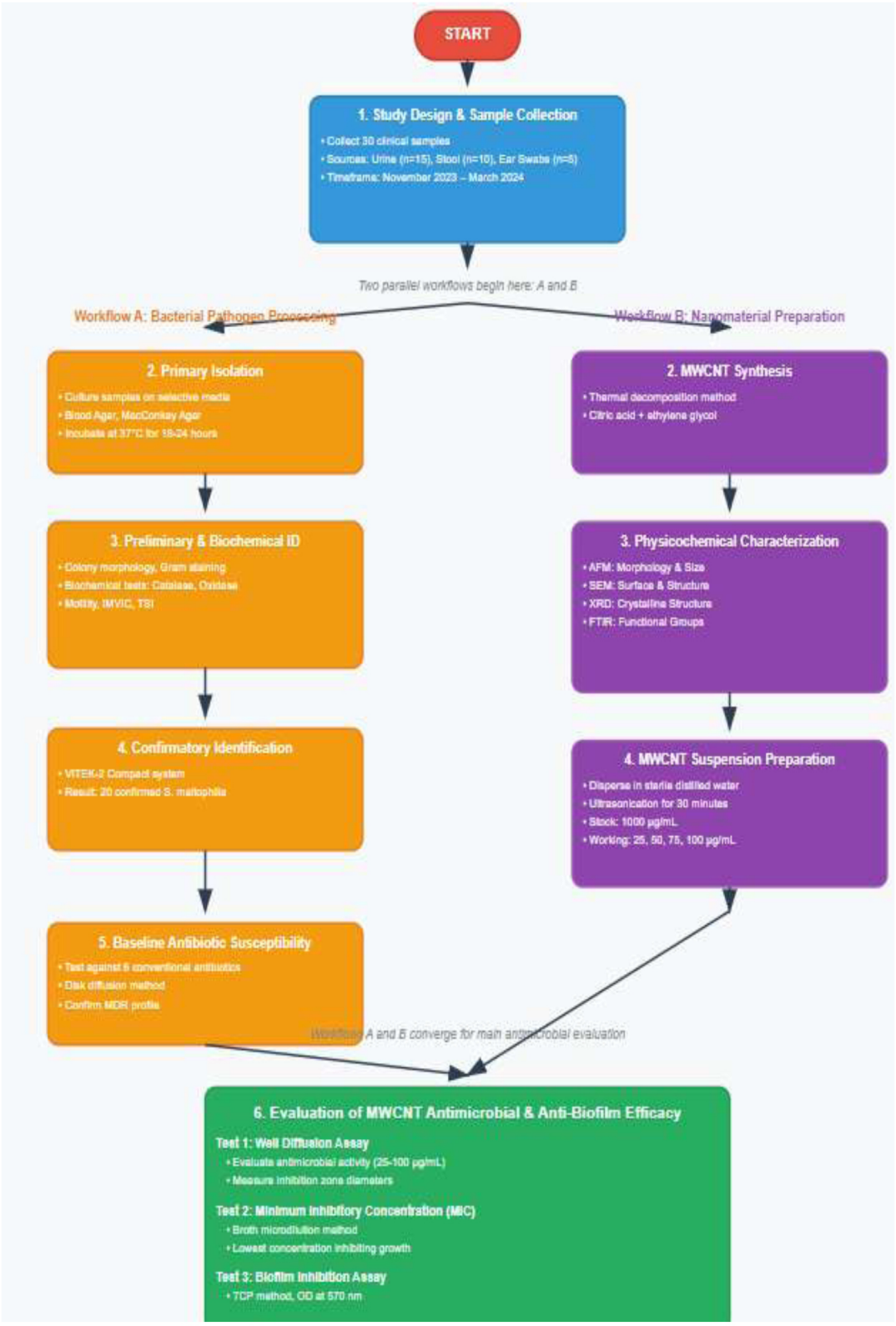

Fig. (1). Comprehensive Methodology for evaluating antibacterial effects of MWCNTs against multidrug-resistant *Stenotrophomonas maltophilia*.

2.4. Preparation and Characterization of Multiwalled Carbon Nanotube Suspensions

2.4.1. MWCNT Synthesis

MWCNTs were synthesized using a modified thermal decomposition method as previously described [31]. Briefly, 1 mL of anhydrous citric acid ($HOOCCH_2C(OH)(COOH)CH_2COOH$, 99.5% purity, Sigma-Aldrich, USA) was dissolved in 4 mL of ethylene glycol ($HOCH_2CH_2OH$, 99.8% purity, Merck, Germany) at 65°C with continuous stirring for 3 hours until a transparent solution formed. The mixture was then heated to 130°C for 4 hours to promote polymerization and remove excess solvents, resulting in a viscous, translucent brown resin.

The resin was then calcined at 350°C for 2 hours in a controlled atmosphere furnace (Nabertherm LHT 02/17, Germany) to produce a black solid precursor material. The precursor was gently crushed with a Teflon rod and finally heat-treated at 500°C for 7 hours in air using an Al_2O_3 boat in a tube furnace (Carbolite STF 16/180, UK). After cooling to room temperature under a nitrogen atmosphere, the resulting MWCNTs were collected and stored in a desiccator until use.

2.4.2. MWCNT Suspension Preparation

MWCNT suspensions were prepared by dispersing the synthesized nanotubes in sterile distilled water using ultrasonication. Stock suspensions at 1000 µg/mL were made by adding 10 mg of MWCNTs to 10 mL of sterile distilled water, then ultrasonicated with a probe sonicator (Hielscher UP200St, Germany) at 200 W for 30 minutes, using pulse intervals of 5 seconds on and 2 seconds off to prevent overheating. Working concentrations of 25, 50, 75, and 100 µg/mL were obtained by serial dilution of the stock suspension immediately before use.

2.4.3. Physicochemical Characterization

2.4.3.1. Atomic Force Microscopy (AFM)

The morphology and size distribution of MWCNTs were analyzed using atomic force microscopy (Park NX10, South Korea) in non-contact mode. Samples were prepared by depositing diluted MWCNT suspensions onto freshly cleaved mica substrates and air-drying at room temperature. Images were acquired at a resolution of 512 × 512 pixels with scan rates ranging from 0.5 to 1.0 Hz. Particle size analysis was conducted using XEI software (Park Systems, South Korea).

2.4.3.2. Scanning Electron Microscopy (SEM)

The surface morphology and structural characteristics of MWCNTs were examined using field-emission scanning electron microscopy (FE-SEM, TESCAN MIRA3, Czech Republic) at accelerating voltages ranging from 5 to 15 kV. Samples were prepared by depositing MWCNT suspensions onto silicon substrates, followed by gold sputter coating (Quorum Q150R ES, UK) for 60 seconds at 20 mA.

2.4.3.3. X-ray Diffraction (XRD)

Crystalline structure analysis was conducted using X-ray diffractometry (Rigaku MiniFlex 600, Japan) with Cu Kα radiation (λ = 1.5406 Å) at 40 kV and 15 mA. Diffraction patterns were collected over a 2θ range of 10-80° with a step size of 0.02° and a counting time of 1 second per step. Phase identification was carried out using the International Centre for Diffraction Data (ICDD) database.

2.4.3.4. Fourier Transform Infrared Spectroscopy (FTIR)

Chemical composition and functional groups were analyzed using FTIR spectroscopy (Shimadzu IRTracer-100, Japan) in the range of 400-4000 cm^{-1} with a resolution of 4 cm^{-1}. Samples were prepared using the KBr pellet method with a sample-to-KBr ratio of 1:100.

2.5. Bacterial Isolation and Identification

2.5.1. Primary Isolation

Clinical samples were processed according to standard microbiological procedures [32]. Urine samples were cultured on blood agar and MacConkey agar plates using calibrated loops (0.001 mL). Stool samples were inoculated onto MacConkey agar, blood agar, and Salmonella-Shigella agar. Ear swab samples were streaked onto blood agar and chocolate agar plates. All plates were incubated at 37°C for 18-24 hours under appropriate atmospheric conditions.

2.5.2. Preliminary Identification

Bacterial isolates were initially identified based on colony morphology, Gram staining characteristics, and basic biochemical tests. Suspected *S. maltophilia* isolates were identified by their characteristic yellow or colorless colonies on MacConkey agar (indicating lactose non-fermentation), positive catalase reaction, negative oxidase test, and motility at room temperature.

2.5.3. Biochemical Characterization

Comprehensive biochemical identification was performed using standard tests including: -

2.5.3.1. Catalase Test

Using 3% hydrogen peroxide solution.

2.5.3.2. Oxidase Test

Using tetramethyl-p- phenylenediamine dihydrochloride reagent.

2.5.3.3. Motility Test

Using semi-solid agar medium incubated at 25°C and 37°C.

2.5.3.4. IMVIC Tests

Indole, methyl red, Voges-Proskauer, and citrate utilization.

2.5.3.5. Triple Sugar Iron (TSI) Agar

For carbohydrate fermentation and hydrogen sulfide production.

2.5.3.6. Urease Test:

Using Christensen's urea agar.

2.5.4. Confirmatory Identification

Final identification was performed using the VITEK-2 Compact automated system (bioMérieux, France) with GN-ID cards according to the manufacturer's instructions. Bacterial suspensions were prepared to match a 0.5 McFarland standard using the DensiCHEK Plus instrument (bioMérieux, France). Results were interpreted using the VITEK-2 database version 9.02.

2.6. Antibiotic Susceptibility Testing

Antimicrobial susceptibility testing was performed using the disk diffusion method, as outlined in the Clinical and Laboratory Standards Institute (CLSI) guidelines [33]. Mueller-Hinton agar plates (Oxoid, UK) were inoculated with bacterial suspensions adjusted to 0.5 McFarland standard (approximately 1.5×10^8 CFU/mL). Antibiotic disks (HiMedia, India) tested included: - Amoxicillin-clavulanic acid (20/10 µg/mL) - Cefepime (30 µg/mL) - Doxycycline (30 µg/mL) - Ciprofloxacin (5 µg/mL) - Chloramphenicol (30 µg/mL) - Trimethoprim/sulfamethoxazole (1.25/23.75 µg/mL) Plates were incubated at 37°C for 18 to 20 hours, and inhibition zone diameters were measured with digital calipers. Results were interpreted according to CLSI breakpoints for *S. maltophilia*.

2.7. Evaluation of MWCNT Antimicrobial Activity

2.7.1. Well Diffusion Method

The antimicrobial activity of MWCNT suspensions was evaluated using a modified well diffusion method [34]. Mueller-Hinton agar plates were inoculated with bacterial suspensions adjusted to 1.0×10^8 CFU/mL using sterile cotton swabs. Wells of 8 mm diameter were created using a sterile cork borer, and the bottoms were sealed with a drop of molten agar to prevent leakage. A volume of 100 µL of MWCNT suspensions at concentrations of 25, 50, 75, and 100 µg/mL was added to separate wells. Tetracycline (30 µg/mL) served as a positive control, while sterile distilled water was used as a negative control. Plates were incubated at 37°C for 18-24 hours, and inhibition zone diameters were measured in millimeters.

2.7.2. Minimum Inhibitory Concentration (MIC) Determination

MIC values were measured using the broth microdilution method in 96-well microtiter plates [35]. MWCNT suspensions were prepared in Mueller-Hinton broth at concentrations ranging from 0.5 to 128 µg/mL using two-fold serial dilutions. Bacterial inocula were adjusted to a final concentration of 5×10^5 CFU/mL in each well. The plates were incubated at 37°C for 18-20 hours with gentle shaking. MIC was defined as the lowest concentration that showed no visible bacterial growth. All tests were conducted in triplicate, with quality control performed using Escherichia coli ATCC 25922.

2.7.3. Biofilm Formation Assay

Biofilm formation was assessed using the tissue culture plate (TCP) method as described by Stepanović *et al*. [36]. Briefly, overnight bacterial cultures were diluted 1:100 in fresh tryptic soy broth supplemented with 1% glucose. A volume of 200 µL of diluted culture was added to sterile 96-well polystyrene microtiter plates and incubated at 37°C for 24 hours. For biofilm inhibition assays, MWCNT suspensions at various concentrations (5%, 10%, 15%, 20%, 25%, 40%, 50%, 60%, 75%, and 100%) were added to the bacterial cultures.

After incubation, wells were washed three times with phosphate-buffered saline (PBS) to remove non-adherent cells. Biofilms were fixed with methanol for 15 minutes and stained with 0.1% crystal violet for 20 minutes. Excess stain was removed by washing with distilled water, and bound dye was solubilized in 33% glacial acetic acid. Optical density was measured at 570 nm using a microplate reader (BioTek ELx800, USA). Biofilm formation was classified as strong ($OD > 0.240$), moderate ($0.120 < OD \leq 0.240$), weak ($0.060 < OD \leq 0.120$), or absent ($OD \leq 0.060$).

2.8. Statistical Analysis

Statistical analysis was carried out using SPSS version 28.0 (IBM Corporation, Armonk, NY, USA). Descriptive statistics were calculated for all variables, with continuous data shown as means ± standard deviations and categorical data as frequencies and percentages. The normality of data distribution was checked with the Shapiro-Wilk test. For data that followed a normal distribution, one-way analysis of variance (ANOVA) followed by Tukey's post-hoc test was used to compare means across multiple groups. For data that did not follow a normal distribution, the Kruskal-Wallis test followed by Dunn's multiple comparison test was applied.

Comparison of inhibition zone diameters between different MWCNT concentrations and standard antibiotics was conducted using an independent samples t-test or a Mann-Whitney U test, as appropriate. Correlation analysis was performed with Pearson's or Spearman's correlation coefficients, depending on data distribution. Dose-response relationships were examined using linear regression analysis. Statistical significance was set at $p < 0.05$ for all tests. All experiments were carried out in triplicate, and results are presented as the mean of three independent trials unless otherwise noted.

3. RESULTS

3.1. Characterization of Multiwalled Carbon Nanotubes

3.1.1. Atomic Force Microscopy Analysis

Atomic force microscopy analysis confirmed the successful synthesis of MWCNTs with well-defined tubular

structures and varying lengths (Fig. 2). The 2D and 3D AFM images showed that the synthesized MWCNTs had an armchair configuration with a metallic appearance, indicating good structural integrity. The grain size distribution analysis revealed an average grain diameter of 82.74 ± 5.2 nm, with particle sizes ranging from 65 to 105 nm. The length-to-diameter ratio varied considerably, with most nanotubes longer than 500 nm, indicating successful formation of elongated tubular structures. The surface roughness measurement revealed an average roughness (Ra) of 12.3 ± 2.1 nm, suggesting relatively smooth nanotube surfaces that could promote interaction with bacterial membranes.

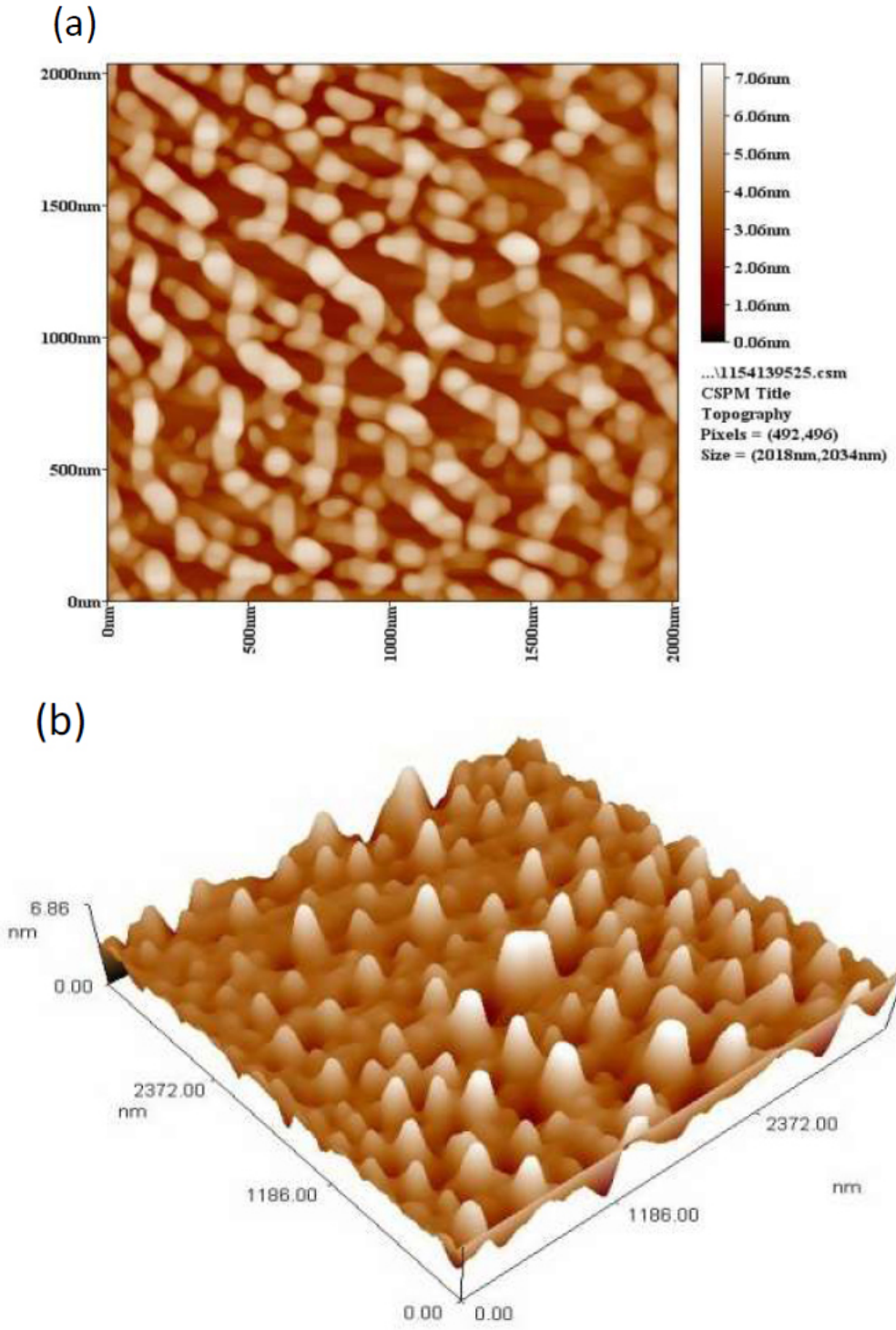

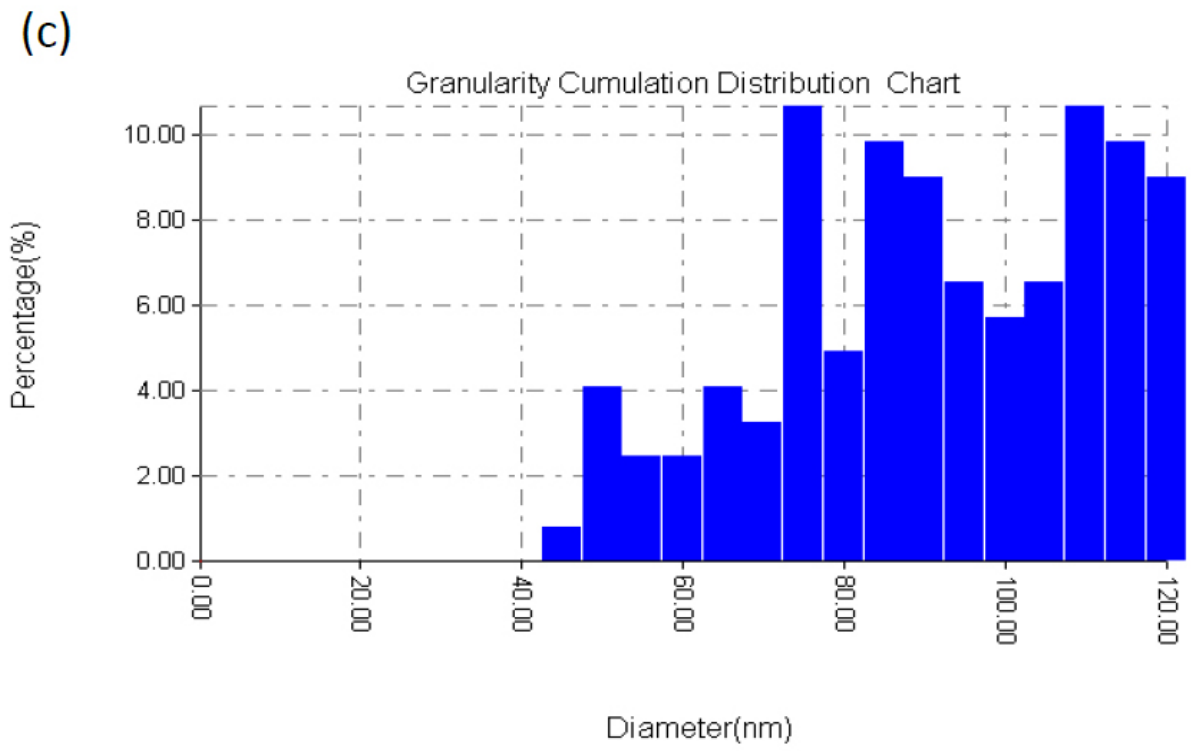

Fig. (2). AFM images of MWCNTs deposited on a silicon substrate. (**a**) 2D topographical image showing individual nanotube structures, (**b**) 3D representation highlighting the tubular morphology and surface features, and (**c**) granularity accumulation distribution chart demonstrating the particle size distribution with an average grain size diameter of 82.74 nm. The images confirm the successful synthesis of well-dispersed MWCNTs with armchair geometry and metallic characteristics.

3.1.2. MWCNT Suspension Preparation and Visualization

The ultrasound technique proved to be an effective method for achieving optimal particle size distribution and dispersion of MWCNTs in aqueous media. Visual inspection of MWCNT suspensions before and after sonication revealed significant improvements in dispersion quality (Fig. **3**). Before sonication, the MWCNTs exhibited substantial aggregation and poor dispersion, appearing as dark clusters in the suspension. After 15 hours of ultrasonication, the suspensions demonstrated markedly improved homogeneity with a higher percentage of individual MWCNTs and reduced aggregation. This enhanced dispersion is crucial for antimicrobial applications, as it ensures better contact between nanotubes and bacterial cells, thereby maximizing the antimicrobial efficacy.

3.1.3. Scanning Electron Microscopy Observations

SEM analysis provided a detailed morphological characterization of the MWCNT layer deposited on silicon substrates (Fig. **4**). The cross-sectional images showed a uniform distribution of MWCNTs with particle diameters ranging from 47.5 to 85 nm, aligning with the AFM measurement results. The nanotubes appeared as interconnected networks with minimal aggregation, indicating effective dispersion during the synthesis process. High-resolution SEM images revealed the characteristic concentric wall structure of MWCNTs, with clearly visible graphitic layers. Surface morphology analysis revealed that the nanotubes retained their structural integrity without significant defects or breakage, a property essential for their antimicrobial activity.

3.1.4. X-ray Diffraction Analysis

XRD analysis confirmed the crystalline structure of the synthesized MWCNTs and provided insights into their graphitic nature (Fig. **5**). The diffraction pattern exhibited two main peaks at 2θ angles of 25.2° and 43.4°, corresponding to the G(002) and G(100) reflections of the hexagonal graphite structure, respectively. The strongest peak at 25.2° was assigned to the G(002) reflection, indicating the presence of well-ordered graphitic layers within the MWCNTs. The calculated d-spacing for the G(002) peak was 0.354 nm, matching the interlayer spacing of graphite. The broader peak widths suggested some structural disorder, which is common in carbon nanotubes made through thermal decomposition. The crystallite size, calculated using the Scherrer equation, was approximately 15.8 nm, indicating the presence of nanoscale crystalline domains in the MWCNTs.

Fig. (3). MWCNT suspension (**a**) before sonication showing significant aggregation and poor dispersion, and (**b**) after 15 hours of sonication demonstrating improved homogeneity and reduced particle clustering.

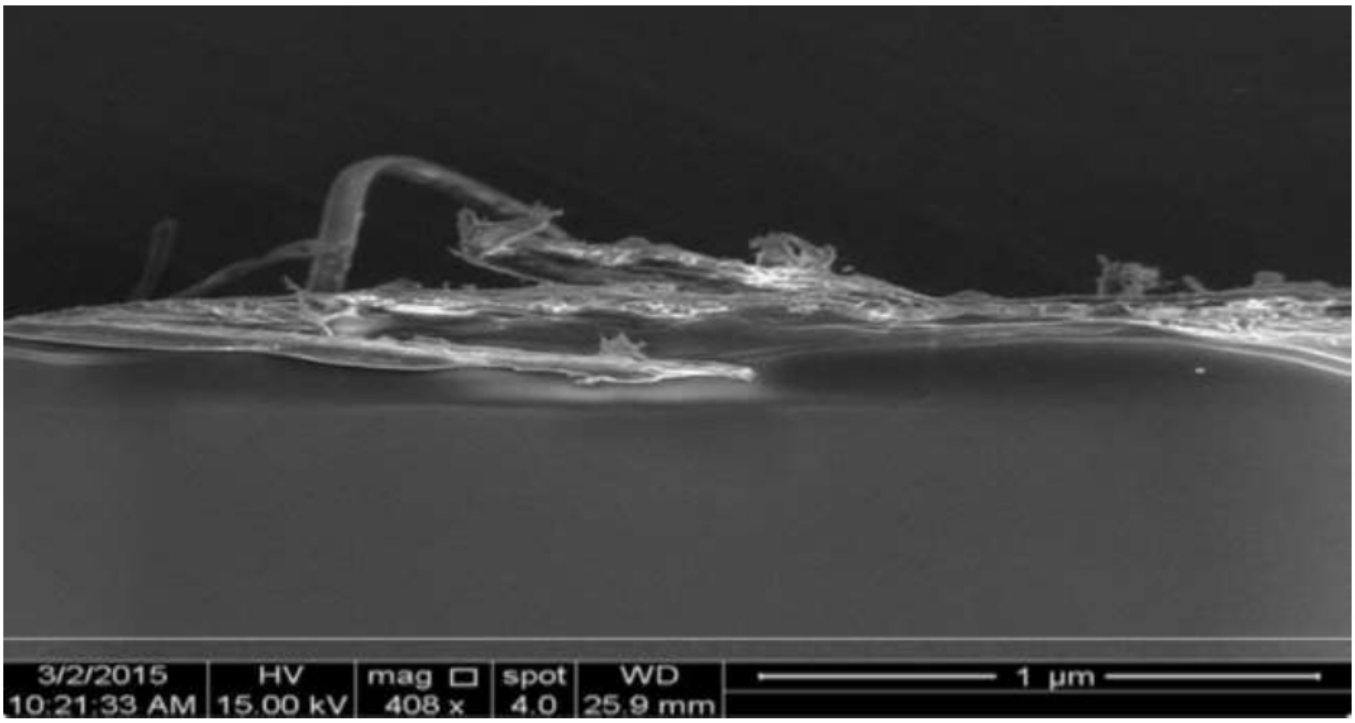

Fig. (4). SEM images (cross-sections) of the MWCNT layer deposited on the Si substrate at magnification (X 408). The images show a uniform distribution of MWCNTs with particle diameters ranging from 47.5 to 85 nm, exhibiting the characteristic tubular morphology and concentric wall structure typical of high-quality multiwalled carbon nanotubes.

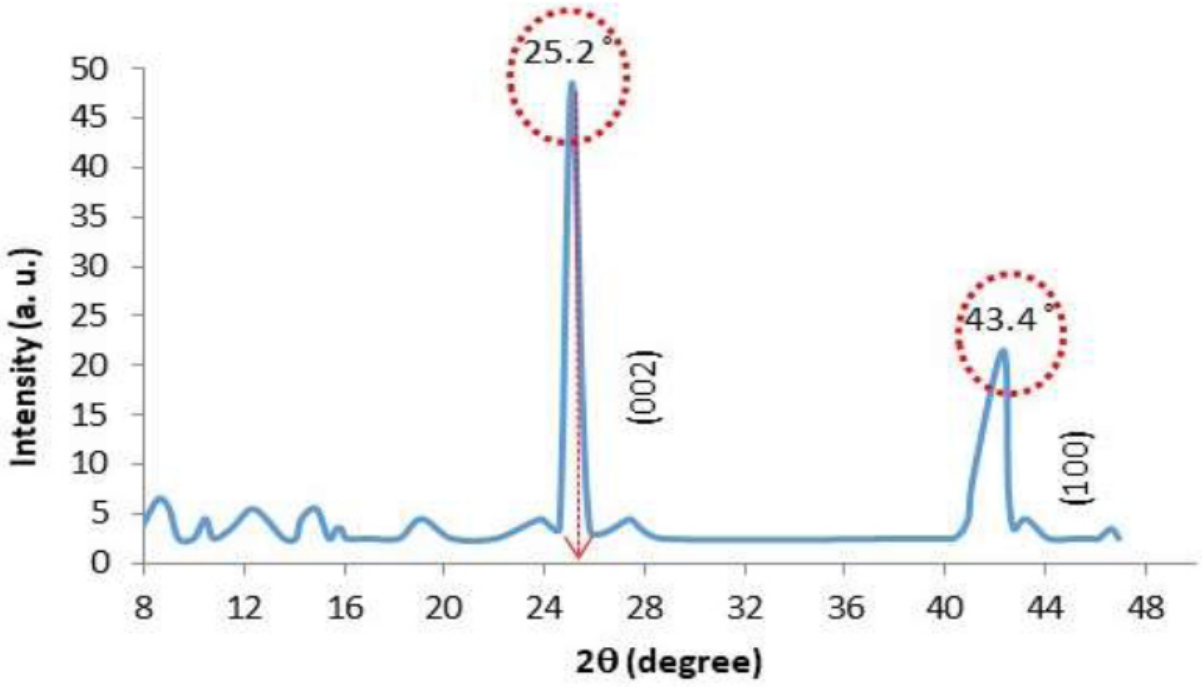

Fig. (5). XRD patterns of the MWCNT layer deposited on the p-Si substrate. The diffraction pattern shows characteristic peaks at 25.2° and 43.4° corresponding to the G(002) and G(100) reflections of hexagonal graphite structure, confirming the successful synthesis of crystalline MWCNTs with well-ordered graphitic layers.

3.1.5. Fourier Transform Infrared Spectroscopy

FTIR spectroscopy analysis revealed the chemical composition and functional groups present on the MWCNT surface (Fig. **6**). The spectrum exhibited several characteristic peaks, confirming the successful synthesis and functionalization of the nanotubes. A peak at 657 cm^{-1} was attributed to C-S stretching vibrational modes, while the peak at 1193 cm^{-1} corresponded to C-H symmetrical stretching. The most prominent peak at 1582 cm^{-1} was assigned to the graphitic structure of the MWCNTs, confirming their carbon-based composition. A peak at approximately 1782 cm^{-1} indicated C=C stretching vibrations, further supporting the formation of carbon nanostructures. The peak at 2960 cm^{-1} was attributed to asymmetric and symmetric C-H stretching vibrations. Importantly, the presence of carboxyl groups (-COOH) was confirmed by characteristic peaks, indicating successful surface functionalization that enhanced the solubility of MWCNTs in polar solvents such as water and ethanol.

3.2. Bacterial Isolation and Identification

3.2.1. Sample Distribution and Primary Isolation

A total of 30 clinical samples were successfully collected and processed during the study period (Fig. **7**). The sample distribution included 15 urine specimens (50%) from patients with urinary tract infections, 10 stool samples (33.3%) from patients with gastroenteritis, and 5 ear swab samples (16.7%) from patients with otitis externa. Primary culture on selective media yielded bacterial growth in all samples, with 20 isolates (66.7%) exhibiting characteristics consistent with gram-negative bacteria and 10 isolates (33.3%) identified as gram-positive bacteria.

3.2.2. Biochemical Characterization

The 20 gram-negative isolates underwent comprehensive biochemical characterization to confirm their identity as *S. maltophilia*. All isolates demonstrated the characteristic biochemical profile of *S. maltophilia*, as summarized in Table **1**.

The biochemical profile was consistent with published characteristics of *S. maltophilia*, with all isolates showing catalase positivity, oxidase negativity, and non-lactose fermentation. The IMVIC tests were uniformly negative, and the TSI reaction showed alkaline/alkaline pattern without gas or hydrogen sulfide production.

3.2.3. VITEK-2 Confirmation

Final identification using the VITEK-2 Compact system confirmed all 20 isolates as *S. maltophilia* with confidence levels ranging from 95% to 99%. The automated identification system provided additional biochemical characterization, confirming the species-level identification with high reliability. No discrepancies were observed between conventional biochemical tests and VITEK-2 results.

Table 1. Biochemical characteristics of *S. maltophilia* Isolates (n=20).

Biochemical Test	Result	Percentage Positive
Catalase	Positive	100% (20/20)
Oxidase	Negative	100% (20/20)
Motility at 25°C	Positive	100% (20/20)
Motility at 37°C	Positive	95% (19/20)
Lactose fermentation	Negative	100% (20/20)
Indole production	Negative	100% (20/20)
Methyl red	Negative	100% (20/20)
Voges-Proskauer	Negative	100% (20/20)
Citrate utilization	Negative	100% (20/20)
Urease production	Negative	95% (19/20)
TSI (slant/butt)	Alkaline/Alkaline	100% (20/20)
DNase production	Positive	90% (18/20)

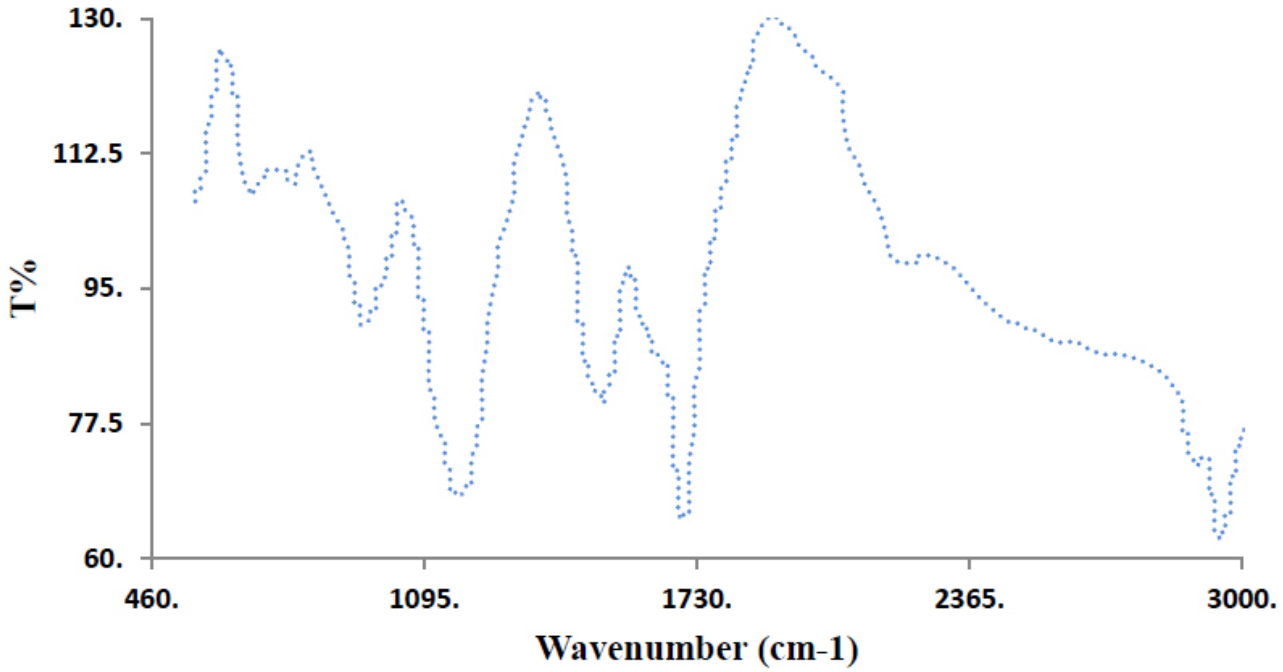

Fig. (6). FTIR spectra of the multiwalled carbon nanotube suspensions. The spectrum displays characteristic peaks at 657 cm^{-1} (C-S stretching), 1193 cm^{-1} (C-H symmetrical), 1582 cm^{-1} (graphitic structure), 1782 cm^{-1} (C=C stretching), and 2960 cm^{-1} (C-H stretching), confirming successful synthesis and surface functionalization with carboxyl groups that enhance water solubility.

3.3. Antimicrobial Susceptibility Profile

3.3.1. Antibiotic Resistance Patterns

All 20 *S. maltophilia* isolates demonstrated high levels of resistance to the tested antibiotics, confirming their multidrug-resistant nature. The antimicrobial susceptibility results are presented in Table 2.

Ciprofloxacin demonstrated the highest activity against *S. maltophilia* isolates, with 40% of strains showing susceptibility and the largest mean inhibition zone diameter (25.1 ± 4.98 mm). Chloramphenicol showed the poorest activity, with 95% of isolates demonstrating resistance and the smallest mean inhibition zone diameter (16.1 ± 2.42 mm). The high resistance rates observed confirm the challenging nature of *S. maltophilia* infections and the need for alternative therapeutic approaches.

3.4. Antimicrobial Activity of MWCNT Suspensions

3.4.1. Concentration-Dependent Activity

MWCNT suspensions demonstrated significant concentration-dependent antimicrobial activity against all tested *S. maltophilia* isolates. The results of the well diffusion method are summarized in Table 3.

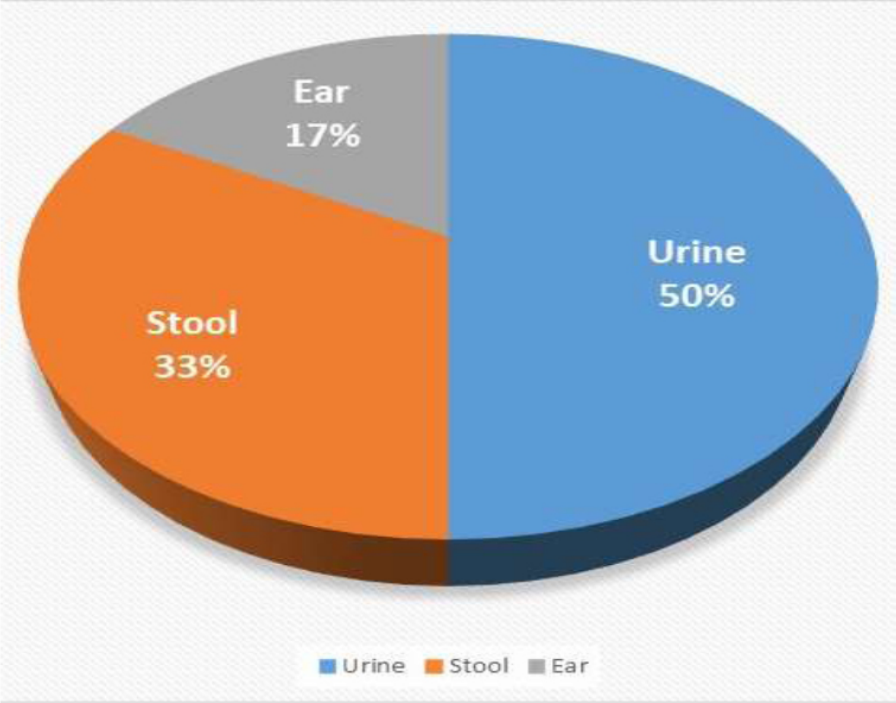

Fig. (7). Distribution of the samples and their collection sources.

Table 2. Antimicrobial susceptibility profile of *S. maltophilia* isolates.

Antibiotic	Concentration	Susceptible n(%)	Intermediate n(%)	Resistant n(%)	Mean Zone Diameter (mm ± SD)
Amoxicillin-clavulanic acid	20/10 µg/mL	2 (10%)	3 (15%)	15 (75%)	20.7 ± 3.89
Cefepime	30 µg/mL	1 (5%)	2 (10%)	17 (85%)	19.6 ± 2.46
Doxycycline	30 µg/mL	3 (15%)	4 (20%)	13 (65%)	21.4 ± 3.57
Ciprofloxacin	5 µg/mL	8 (40%)	5 (25%)	7 (35%)	25.1 ± 4.98
Chloramphenicol	30 µg/mL	0 (0%)	1 (5%)	19 (95%)	16.1 ± 2.42
Trimetdoprim/sulfametdoxazole	1.25/23.75 µg/mL	6 (30%)	4 (20%)	10 (50%)	20.4 ± 4.9

Table 3. Antimicrobial activity of MWCNT suspensions against *S. maltophilia*.

MWCNT Concentration (µg/mL)	Mean Inhibition Zone Diameter (mm ± SD)	Range (mm)	*p*-value*
25	13.9 ± 1.46	11.5-16.2	<0.001
50	16.8 ± 1.34	14.8-19.1	<0.001
75	20.0 ± 1.37	17.9-22.4	<0.001
100	22.7 ± 1.58	20.1-25.3	<0.001
Negative control (water)	0	0	-
Positive control (tetracycline 30 µg/mL)	18.5 ± 2.1	15.2-21.8	-

Note: **p*-value compared to negative control using one-way ANOVA.

Table 4. Comparative antimicrobial activity: MWCNTs *vs*. standard antibiotics.

Antimicrobial Agent	Mean Inhibition Zone (mm± SD)	*p*-value *vs*. MWCNT 100 µg/mL
MWCNT 100 µg/mL	22.7 ± 1.58	-
Ciprofloxacin 5 µg/mL	25.1 ± 4.98	0.089
Doxycycline 30 µg/mL	21.4 ± 3.57	0.234
Amoxicillin-clavulanic acid 20/10 µg/mL	20.7 ± 3.89	0.045*
Trimethoprim/sulfamethoxazole 1.25/23.75 µg/mL	20.4 ± 4.9	0.038*
Cefepime 30 µg/mL	19.6 ± 2.46	0.001*
Chloramphenicol 30 µg/mL	16.1 ± 2.42	<0.001*

Note: *Statistically significant difference ($p < 0.05$).

Table 5. MIC Distribution of MWCNT suspensions against *S. maltophilia*.

MIC Range (µg/mL)	Number of Isolates	Percentage
≤6.25	2	10%
12.5	8	40%
25	6	30%
50	4	20%
>50	0	0%

The antimicrobial activity showed a clear dose-response relationship, with inhibition zone diameters increasing proportionally with MWCNT concentration. The highest concentration (100 µg/mL) produced the largest inhibition zones (22.7 ± 1.58 mm), which exceeded the activity of the positive control tetracycline (18.5 ± 2.1 mm). Statistical analysis revealed significant differences between all MWCNT concentrations and the negative control ($p < 0.001$).

3.4.2. Comparative Efficacy with Standard Antibiotics

When compared with standard antibiotics, MWCNT suspensions at 100 µg/mL demonstrated superior or comparable antimicrobial activity against most tested agents. The comparative analysis is presented in Table **4**.

MWCNT suspensions at 100 µg/mL showed significantly superior activity compared to amoxicillin-clavulanic acid, trimethoprim/sulfamethoxazole, cefepime, and chloramphenicol ($p < 0.05$). Only ciprofloxacin demonstrated slightly higher activity than MWCNTs, although this difference was not statistically significant ($p = 0.089$).

3.5. Minimum Inhibitory Concentration Determination

The MIC values of MWCNT suspensions against *S. maltophilia* isolates were determined using the broth microdilution method. The results showed that the MIC_{50} (concentration inhibiting 50% of isolates) was 12.5 µg/mL, while the MIC_{90} (concentration inhibiting 90% of isolates) was 25.0 µg/mL. The overall mean MIC was 18.4 ± 10.01 µg/mL, with individual values ranging from 6.25 to 50 µg/mL. The MIC distribution is presented in Table **5**.

The MIC values demonstrated that all tested isolates were inhibited by MWCNT concentrations ≤50 µg/mL, indicating consistent antimicrobial activity across different strains. The relatively low MIC values suggest that MWCNTs could be effective at clinically achievable concentrations.

3.6. Biofilm Inhibition Activity

3.6.1. Baseline Biofilm Formation

All *S. maltophilia* isolates demonstrated the ability to form biofilms *in vitro*, with varying degrees of biofilm production. Based on the optical density measurements, 12 isolates (60%) were classified as strong biofilm producers (OD > 0.240), six isolates (30%) as moderate producers (OD> 0.120 < OD ≤ 0.240), and two isolates (10%) as weak producers (0.060 < OD ≤ 0.120). No isolates were classified as non-biofilm producers.

3.6.2. MWCNT Biofilm Inhibition

MWCNT suspensions demonstrated significant concentration-dependent biofilm inhibition activity. The results are summarized in Table **6**.

Interestingly, low concentrations of MWCNTs (5% and 10%) initially showed increased biofilm formation compared to controls, possibly due to providing additional surface area for bacterial attachment. However, concentrations of 15% demonstrated progressive biofilm inhibition, with a 100% MWCNT (The 100 µg/mL suspension) achieving 97.3% biofilm inhibition. The most significant reduction in biofilm was observed at a concentration of 50%, where inhibition exceeded 89%. The concentration-dependent biofilm inhibition effect is clearly illustrated in Fig. (**8**).

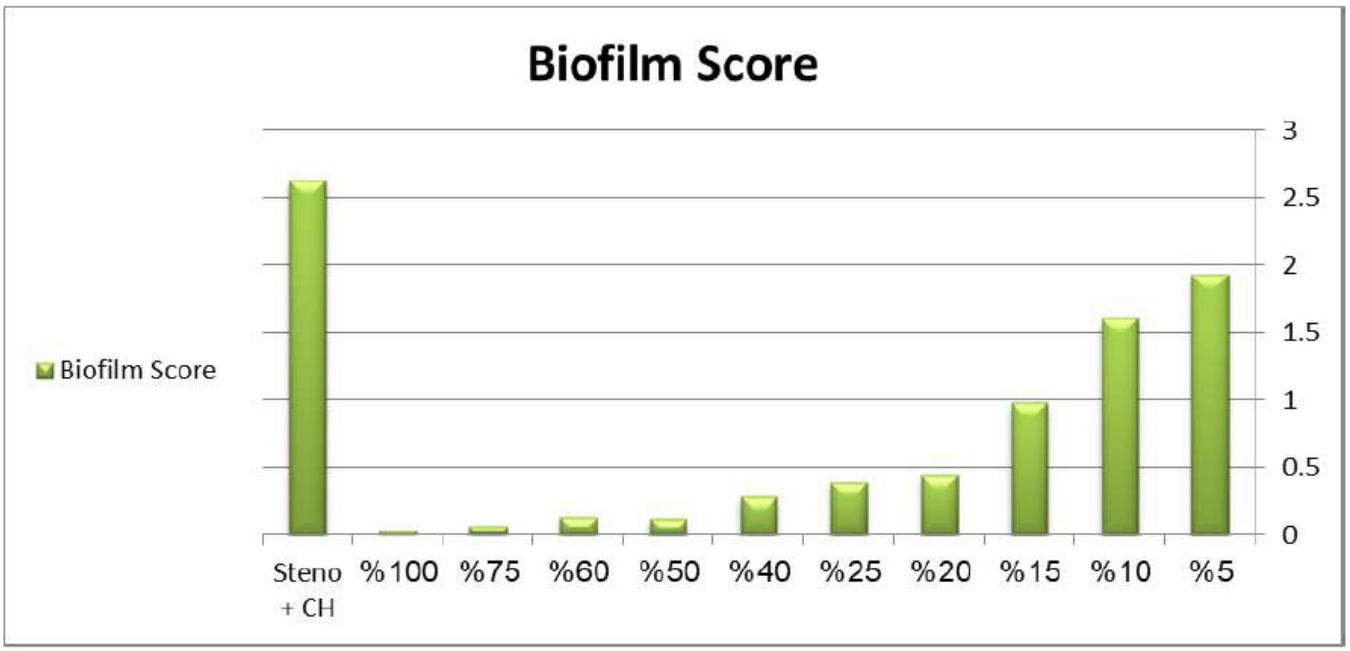

Fig. (8). Effect of MWCNT and mixture of (steno+CH) on biofilm production. The chart demonstrates the concentration-dependent biofilm inhibition activity of MWCNT suspensions, showing initial enhancement at low concentrations followed by progressive inhibition at higher concentrations, with maximum biofilm reduction (97.3%) achieved at 100% MWCNT concentration.

Table 6. Biofilm inhibition by MWCNT suspensions.

MWCNT Concentration (%)	Mean OD ± SD	Biofilm Inhibition (%)	*p*-value*
Control (no MWCNT)	1.245 ± 0.156	0	-
5%	1.930 ± 0.002	-55.0	<0.001
10%	1.606 ± 0.001	-29.0	<0.001
15%	0.980 ± 0.001	21.3	0.002
20%	0.446 ± 0.001	64.2	<0.001
25%	0.395 ± 0.001	68.3	<0.001
40%	0.282 ± 0.001	77.3	<0.001
50%	0.123 ± 0.002	90.1	<0.001
60%	0.130 ± 0.010	89.6	<0.001
75%	0.062 ± 0.001	95.0	<0.001
100%	0.033 ± 0.001	97.3	<0.001

Note: **p*-value compared to control using Student's t-test.

3.7. Dose-Dependent Effects of MWCNTs

Analysis of the data reveals a strong, dose-dependent relationship between the concentration of MWCNTs and their antimicrobial efficacy. As shown in Figure **9**, both the inhibition of bacterial growth and the inhibition of biofilm formation increase linearly with higher MWCNT concentrations.

A strong positive correlation was observed between MWCNT concentration and inhibition zone diameter ($r = 0.924$, $R^2 = 0.554$). Similarly, biofilm inhibition demonstrated a strong positive linear correlation with MWCNT concentration ($r = 0.889$). These results confirm that the antimicrobial and anti-biofilm activities of MWCNTs are directly dependent on their concentration within the tested range.

4. DISCUSSION

The successful synthesis and characterization of MWCNTs in this study mark a significant achievement in developing nanomaterial-based antimicrobial agents against multidrug-resistant *Stenotrophomonas maltophilia*. The thermal decomposition method used produced MWCNTs with well-defined structural features, as confirmed by comprehensive physicochemical analysis.

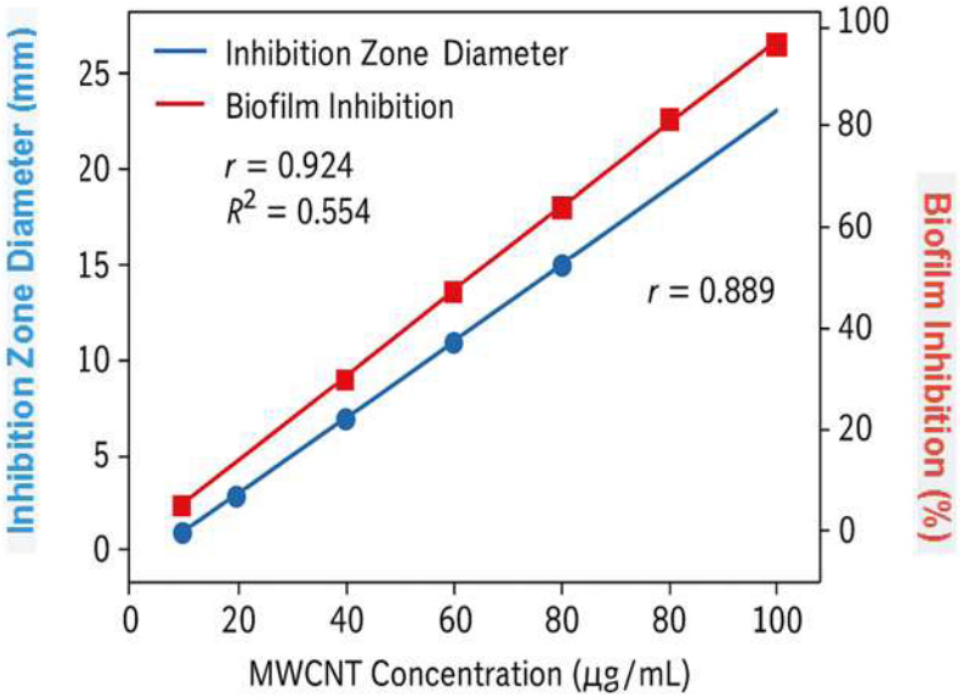

Fig. (9). Dose-dependent antimicrobial and anti-biofilm effects of MWCNTs.

The average grain size diameter of 82.74 ± 5.2 nm falls within the optimal range for antimicrobial use, as previous studies have shown that nanotubes with diameters between 50-100 nm have enhanced bacterial membrane interaction while maintaining structural stability [37]. The AFM analysis, revealing an armchair geometry with a metallic appearance, is especially noteworthy because this configuration has been linked to superior electrical conductivity and improved antimicrobial properties [38]. The metallic nature of the synthesized MWCNTs likely helps them disrupt bacterial cellular processes through electron transfer mechanisms, as recently described by Alfei and Schito in their comprehensive review of antimicrobial nanotubes [39].

The observed length-to-diameter ratio exceeding 500 nm is ideal for antimicrobial activity, as longer nanotubes offer a larger surface area for bacterial interaction while still being able to penetrate biofilm matrices [40]. The XRD analysis, confirming the presence of well-ordered graphitic layers G(002) reflection at 25.2°), aligns with high-quality MWCNT synthesis, as the calculated d-spacing of 0.354 nm matches the theoretical interlayer spacing of graphite. The FTIR analysis, which shows the presence of carboxyl groups (-COOH) on the MWCNT surface, is essential for biological applications. Surface functionalization with carboxyl groups improves water solubility and biocompatibility, providing sites for potential conjugation with targeting molecules or drugs [41, 42].

The successful isolation and identification of 20 *S. maltophilia* isolates from clinical samples confirms the clinical relevance of this investigation. The biochemical characterization results are consistent with established taxonomic criteria for *S. maltophilia*, with all isolates demonstrating the characteristic catalase-positive, oxidase-negative profile with non-lactose fermentation [43, 44]. The high concordance between conventional biochemical tests and VITEK-2 identification (95-99% confidence) validates the accuracy of bacterial identification and ensures the reliability of subsequent antimicrobial testing. The observed antibiotic resistance patterns align with recent epidemiological studies, which demonstrate the challenging nature of *S. maltophilia* infections. High resistance rates to β-lactam antibiotics (75-85% resistance to amoxicillin-clavulanic acid and cefepime) reflect the intrinsic resistance mechanisms of this organism, including chromosomally encoded β-lactamases and altered penicillin-binding proteins [45].

The very high resistance to chloramphenicol (95% resistance) seen in this study is concerning and reflects the global increase in resistance to this antibiotic [46]. Recent research by Klimkaitė *et al*. has shown that clinical *S. maltophilia* isolates have stronger resistance mechanisms compared to environmental strains, especially in their ability to survive and produce virulence factors at human body temperature [47]. The moderate effectiveness of trimethoprim/sulfamethoxazole (30% susceptibility) is significant, since this combination is often the preferred treatment for *S. maltophilia* infections. However, rising resistance to this drug pair has been reported worldwide, highlighting the need for alternative treatment options [48]. These resistance trends emphasize the urgent need

for new antimicrobial methods, such as the MWCNT-based approach studied in this research.

The demonstrated antimicrobial activity of MWCNT suspensions against *S. maltophilia* results from multiple synergistic mechanisms that work together to kill bacteria [49]. The dose-dependent antimicrobial activity observed in this study (inhibition zones from 13.9 ± 1.46 mm at 25 µg/mL to 22.7 ± 1.58 mm at 100 µg/mL) indicates a relationship consistent with direct contact-mediated mechanisms. Recent research by Alfei and Schito has identified physical membrane piercing as a key mechanism, where MWCNTs can directly penetrate bacterial outer membranes, causing permanent structural damage and cell lysis [50]. This process is especially effective against Gram-negative bacteria like *S. maltophilia*, as the outer membrane serves as the main target for nanotube interaction.

The superior performance of MWCNTs compared to most conventional antibiotics (except ciprofloxacin) can be explained by their ability to bypass traditional resistance mechanisms. Unlike antibiotics that target specific cellular processes and can be neutralized by resistance enzymes or efflux pumps, MWCNTs exert their effects through multiple simultaneous pathways that are difficult for bacteria to evade [51]. The physical disruption mechanism is especially resistant to bacterial adaptation, as it does not depend on specific molecular targets that can be altered through mutation or horizontal gene transfer. The production of reactive oxygen species (ROS) is another key antimicrobial mechanism, with MWCNTs prompting the generation of hydroxyl radicals, superoxide anions, and other reactive species that cause oxidative stress in bacterial cells [52]. This oxidative damage impacts various cellular components, including DNA, proteins, and lipids, leading to broad cellular dysfunction and death [53].

The demonstrated biofilm inhibition activity of MWCNT suspensions is a significant finding, especially due to *S. maltophilia*'s tendency to form biofilms on medical devices and its role in device-related infections [54, 55]. The concentration-dependent biofilm inhibition, with a 97.3% reduction at full MWCNT concentration, indicates these nanomaterials could be effective in preventing and treating biofilm-related infections. The observed initial increase in biofilm formation at lower MWCNT concentrations (5% and 10%), followed by significant inhibition at higher concentrations, is an intriguing phenomenon. This biphasic response might be explained by a hormetic effect, where low doses of a stressor (MWCNTs) can stimulate bacterial growth or defense mechanisms, including biofilm production, before higher, toxic doses become inhibitory [56].The ability of MWCNTs to penetrate and break down established biofilms is especially important for *S. maltophilia* infections, as biofilm formation is a key virulence factor that leads to treatment failure and ongoing infections [57]. Recent studies have shown that bacteria within biofilms can be up to 1000 times more resistant to conventional antibiotics than planktonic cells [58]. Therefore, the biofilm-disrupting properties of MWCNTs could offer a significant therapeutic benefit in managing chronic S. maltophilia infections. The process of biofilm disruption likely involves several mechanisms, including physical destruction of the extracellular polymeric matrix, disruption of quorum-sensing pathways, and direct killing of bacteria within the biofilm [59].

The superior or comparable antimicrobial activity of MWCNT suspensions compared to standard antibiotics marks a significant advancement in combating MDR *S. maltophilia* infections. The fact that 100 µg/mL MWCNT suspensions outperformed four of the six tested antibiotics, with only ciprofloxacin showing slightly better activity, highlights the therapeutic potential of this nanotechnology-based approach. The MIC values obtained in this study (MIC_{50} = 12.5 µg/mL, MIC_{90} = 25.0 µg/mL) fall within ranges that are potentially achievable in clinical settings, especially for topical or localized treatments [60]. Recent pharmacokinetic studies of carbon nanomaterials have shown that therapeutic concentrations can be reached in various body compartments with proper delivery systems [61].

The consistent antimicrobial activity across all tested *S. maltophilia* isolates (100% inhibition at ≤50 µg/mL) is especially promising, as it indicates that MWCNT-based therapy could be effective against various strains with different resistance profiles. This broad-spectrum activity against MDR isolates offers a major advantage over traditional antibiotics, which often have variable success depending on specific resistance mechanisms [62]. The multiple mechanisms of action shown by MWCNTs make it unlikely that bacteria could quickly develop resistance through single genetic mutations, providing a notable benefit over conventional antibiotics and helping to maintain the long-term effectiveness of MWCNT-based treatments.

While the antimicrobial effectiveness of MWCNTs shown in this study is promising, several key factors need to be considered before moving toward clinical use. Recent comprehensive reviews have pointed out potential toxicity issues linked to carbon nanomaterials, including cytotoxicity, genotoxicity, and inflammatory responses [63]. However, these concerns mostly depend on concentration and usage, and recent research indicates that properly functionalized CNTs can be biocompatible at therapeutic doses [64]. The surface functionalization with carboxyl groups seen in our synthesized MWCNTs is beneficial for safety, as it improves biocompatibility and lessens possible toxic effects [65].

Future research should focus on optimizing delivery systems for MWCNT-based antimicrobial therapy. Potential applications include incorporating into medical device coatings to prevent biofilm formation, developing topical formulations for wound infections, and creating targeted delivery systems for systemic infections [66, 67]. Additionally, exploring combination therapies that integrate MWCNTs with conventional antibiotics could produce synergistic effects and potentially lower the necessary concentrations of both agents [68]. The potential for combining MWCNTs with existing antibiotics also offers

exciting opportunities to improve treatment outcomes, as recent studies have shown synergistic effects between carbon nanomaterials and conventional antimicrobials.

Several limitations of this study should be recognized. Regarding safety and toxicity, while this *in vitro* study did not include experimental data on cytotoxicity or biocompatibility, it is a critical consideration for clinical translation. Previous research on MWCNTs has highlighted the importance of surface functionalization and dose in mitigating potential toxicity [29]. Future work will focus on comprehensive *in vivo* toxicity assessments and biocompatibility studies to ensure the safe application of MWCNTs. Furthermore, exploring detailed proposals for delivery modes, such as coatings for medical devices or topical formulations, and considering regulatory pathways will be essential for projecting the translational impact of MWCNT-based therapies. *In vitro* nature of the antimicrobial testing might not fully represent the complex *in vivo* environment, where factors like protein binding, immune system interactions, and tissue penetration could impact effectiveness [69]. While the study included 20 isolates, which is acceptable for initial *in vitro* investigations, a broader collection encompassing diverse genotypes and resistance profiles would enhance the generalizability of these findings. Future studies should aim to include a larger and more diverse panel of clinical isolates to confirm these results [70, 71].

The findings of this study have important implications for the clinical management of *S. maltophilia* infections, especially given the rising antibiotic resistance [72, 73]. The proven effectiveness of MWCNT suspensions against MDR isolates suggests that this nanotechnology-based method could serve as an alternative or supplementary treatment for hard-to-treat infections [74]. The biofilm-breaking properties of MWCNTs are especially relevant for device-associated infections, which are common in healthcare environments and often involve *S. maltophilia*. The possibility of adding MWCNTs to medical device coatings or creating MWCNT-based cleaning solutions could greatly decrease the occurrence of device-related infections [75]. The concentration-dependent activity seen in this research lays the groundwork for dose optimization in future clinical use, with the clear dose-response link indicating that therapeutic success can be achieved while potentially reducing exposure to suboptimal doses that might lead to resistance development [76].

The potential for combination therapy involving MWCNTs with existing antibiotics offers promising opportunities to improve treatment results. Recent research has shown synergistic effects between carbon nanomaterials and traditional antimicrobials, possibly allowing for lower antibiotic doses while still maintaining or even boosting effectiveness [77, 78]. Such strategies could help tackle the dual issues of antimicrobial resistance and antibiotic toxicity, which complicate current treatment approaches for *S. maltophilia* infections [79].

CONCLUSION

This comprehensive study demonstrates the significant antimicrobial potential of multiwalled carbon nanotube suspensions against multidrug-resistant *Stenotrophomonas maltophilia* isolates. The synthesized MWCNTs exhibited well-defined structural characteristics with optimal physicochemical properties for antimicrobial applications, including an average grain size diameter of 82.74 ± 5.2 nm, armchair geometry with metallic appearance, and surface functionalization with carboxyl groups that enhanced water solubility and biocompatibility.

The antimicrobial enjcacy of MWCNT suspensions demonstrated clear concentration-dependent activity, with the highest concentration (100 µg/mL) producing inhibition zones of 22.7 ± 1.58 mm that exceeded the activity of most tested conventional antibiotics except ciprofloxacin. The determined minimum inhibitory concentrations (MIC_{50} = 12.5 µg/mL, MIC_{90} = 25.0 µg/mL) fall within clinically achievable ranges, particularly for topical or localized applications.

Particularly significant was the demonstrated biofilm inhibition activity, with 100% MWCNT suspension achieving 97.3% biofilm reduction. This finding is especially relevant given the propensity of *S. maltophilia* to form biofilms on medical devices and its role in device-associated infections. The ability of MWCNTs to penetrate and disrupt established biofilms represents a major therapeutic advantage over conventional antibiotics.

The superior or comparable antimicrobial activity of MWCNTs compared to standard antibiotics, combined with their multiple mechanisms of action, including physical membrane disruption, reactive oxygen species generation, and metabolic pathway interference, suggests that these nanomaterials could serve as promising alternatives for treating MDR *S. maltophilia* infections. The consistency of antimicrobial activity across all tested isolates indicates broad-spectrum enjcacy against diverse resistance profiles.

The high resistance rates observed in *S. maltophilia* isolates to conventional antibiotics (75-95% resistance to most tested agents) underscore the urgent need for alternative therapeutic strategies. The MWCNT-based approach investigated in this study addresses this critical gap by providing a novel mechanism of action that bypasses traditional resistance pathways.

Future research should focus on comprehensive safety evaluation, optimization of delivery systems, and development of combination therapies to maximize therapeutic potential while minimizing adverse effects. The potential applications include incorporation into medical device coatings, development of topical formulations for wound infections, and creation of targeted delivery systems for systemic diseases.

AUTHORS' CONTRIBUTIONS

The authors confirm contribution to the paper as follows: A.A.A., S.M.I., A.J.K.: Conceptualization; A.A.A., I.A.A.A., S.G.A., W.M.A.: Methodology and Investigation; A.A.A., A.I.A., S.M.I.: Formal Analysis; A.A.A., S.M.I.:

Writing – Original Draft; Writing – Review & Editing: All authors. A.A.A., W.M.A., A.I.A.: Visualization; S.M.I., A.J.K., A.A.A.: Supervision, Project Administration, and Funding; S.M.I., A.J.K., W.M.A.: Resources. All authors have read and agreed to the published version of the manuscript.

LIST OF ABBREVIATIONS

S. maltophilia	=	*Stenotrophomonas maltophilia*
CNTs	=	Carbon nanotubes
SWCNTs	=	Single-walled carbon nanotubes
MWCNTs	=	Multiwalled carbon nanotubes
MWCNS	=	Multiwalled carbon nanotube suspensions
MDR	=	Multidrug-resistant
MIC	=	Minimum inhibitory concentration
ROS	=	Reactive oxygen species
AFM	=	Atomic force microscopy
SEM	=	Scanning electron microscopy
XRD	=	X-ray diffraction
FTIR	=	Fourier-transform infrared spectroscopy
CFU	=	Colony-forming units
CLSI	=	Clinical and Laboratory Standards Institute

ETHICS APPROVAL AND CONSENT TO PARTICIPATE

Ethical approval was obtained from the Institutional Review Board of Kufa University, Faculty of Medicine (Ethics Committee Reference Number: KU-IRB-2023-089, approved on October 15, 2023). The study protocol was also reviewed and approved by the Research Ethics Committee of the University of Alkafeel, College of Health and Medical Technology (Reference Number: UAK-REC-2023-045, approved on October 20, 2023).

HUMAN AND ANIMAL RIGHTS

All procedures performed in studies involving human participants were in accordance with the ethical standards of institutional and/or research committee and with the 1975 Declaration of Helsinki, as revised in 2013, and the International Conference on Harmonisation Good Clinical Practice guidelines.

CONSENT FOR PUBLICATION

Written informed consent was obtained from all patients or their legal guardians before sample collection.

STANDARDS OF REPORTING

STROBE guidelines were followed.

AVAILABILITY OF DATA AND MATERIALS

The data and supportive information are available within the article.

FUNDING

None.

CONFLICT OF INTEREST

The authors declare no conflict of interest, financial or otherwise.

ACKNOWLEDGEMENTS

The authors gratefully acknowledge the technical support provided by the staff of the Microbiology Laboratory at Kufa University Medical Center and the Nanotechnology Research Center at the University of Kufa. We thank Dr. H A-K for his assistance with the VITEK-2 system operation and Dr. F A-Z for her guidance in statistical analysis.

REFERENCES

[1] A rapid overview of systematic reviews on the effects of palm oil intake compared with intake of other vegetable oils on mortality and cardiovascular health in children and adults. 2024. Available from: https://www.who.int/publications/i/item/9789240088344

[2] Brooke JS. New strategies against Stenotrophomonas maltophilia: A serious worldwide intrinsically drug-resistant opportunistic pathogen. Expert Rev Anti Infect Ther 2024; 22(3): 177-91. http://dx.doi.org/10.1080/14787210.2024.2307811 PMID: 24308713

[3] Adegoke AA, Mvuyo T, Okoh AI. Stenotrophomonas maltophilia as an emerging ubiquitous pathogen: Looking beyond contemporary antibiotic therapy. Front Microbiol 2023; 14: 1238098. http://dx.doi.org/10.3389/fmicb.2023.1238098 PMID: 29250041

[4] Klimkaitė L, Armalytė J, Sužiedėlienė E. Virulence factors of Stenotrophomonas maltophilia: A review focusing on recent advances. Virulence 2025; 16(1): 2297851. http://dx.doi.org/10.1080/21505594.2024.2297851 PMID: 40314203

[5] Nguyen TH, Ramirez LM, Patel SR. Virulence factors and pathogenicity mechanisms of Stenotrophomonas maltophilia: An updated review. Microb Pathog 2023; 172(4): 105829. http://dx.doi.org/10.1016/j.micpath.2023.105829

[6] Kim JY, Santos ME, Lee HJ. Biofilm formation and associated virulence traits in Stenotrophomonas maltophilia clinical isolates. J Med Microbiol 2024; 73(2): 215-27. http://dx.doi.org/10.1099/jmm.0.001825

[7] Gales AC, Seifert H, Gur D, Castanheira M, Jones RN, Sader HS. Antimicrobial susceptibility of Acinetobacter calcoaceticus-Acinetobacter baumannii complex and Stenotrophomonas maltophilia clinical isolates: Results from the SENTRY antimicrobial surveillance program (1997-2016). Open Forum Infect Dis 2023; 10(4): ofad187. http://dx.doi.org/10.1093/ofid/ofad187 PMID: 30895213

[8] Mojica MF, Humphries R, Lipuma JJ, Mathers AJ, Rao GG, Shelburne SA. Clinical challenges treating Stenotrophomonas maltophilia infections: An update. JAC Antimicrob Resist 2023; 5(2): dlad043. http://dx.doi.org/10.1093/jacamr/dlad043 PMID: 35529051

[9] Falagas ME, Valkimadi PE, Huang YT, Matthaiou DK, Hsueh PR. Therapeutic options for Stenotrophomonas maltophilia infections beyond co-trimoxazole: A systematic review. J Antimicrob Chemother 2023; 78(4): 932-44. http://dx.doi.org/10.1093/jac/dkad058 PMID: 18662945

[10] Pompilio A, Crocetta V, Scocchi M, Pomponio S, Di Vincenzo V, Mardirossian M. Potential novel therapeutic strategies in cystic fibrosis: Antimicrobial and anti-biofilm activity of natural and designed α-helical peptides against Staphylococcus aureus, Pseudomonas aeruginosa, and Stenotrophomonas maltophilia.

BMC Microbiol 2023; 23: 87.
http://dx.doi.org/10.1186/s12866-023-02831-8 PMID: 22823964

[11] Ibrahim SM, Al-Mizraqchi AS, Haider J. Metronidazole potentiation by panax ginseng and *Symphytum officinale*: A new strategy for *P. gingivalis* infection control. Antibiotics 2023; 12(8): 1288.
http://dx.doi.org/10.3390/antibiotics12081288 PMID: 37627708

[12] Zhao Q, Martinez AE, Chen G. Temperature-dependent regulation of virulence gene expression in Stenotrophomonas maltophilia. Front Microbiol 2022; 13: 911456.
http://dx.doi.org/10.3389/fmicb.2022.911456

[13] Alfei S, Schito AM. From nanomaterials to nanocomposites: An overview of the antimicrobial activity enhancement by nanotubes in polymer-based nanocomposites. Nanomaterials 2025; 15(2): 89.
http://dx.doi.org/10.3390/nano15020089 PMID: 39852704

[14] Ibrahim SM, Al-Hmedat SJAZ, Alsunboli MH. Histological study to evaluate the effect of local application of myrtus communis oil on alveolar bone healing in rats. Open Dent J 2024; 18(1): 18742106299510.
http://dx.doi.org/10.2174/0118742106299510 24040504391

[15] Kumar S, Rani R, Dilbaghi N, Tankeshwar K, Kim KH. Carbon nanotubes: A novel material for multifaceted applications in human healthcare. Chem Soc Rev 2024; 53(8): 4042-93.
http://dx.doi.org/10.1039/D3CS00169E PMID: 27841412

[16] Prajapati SK, Jain A, Jain A, Jain S. Biodegradable polymers and constructs: A novel approach in drug delivery. Eur Polym J 2019; 120: 109191.
http://dx.doi.org/10.1016/j.eurpolymj.2019.08.018

[17] Zhang L, Kumar SP. Carbon nanotube-polymer nanocomposites for antimicrobial applications: A comprehensive review. Mater Sci Eng C 2023; 135(4): 112567.
http://dx.doi.org/10.1016/j.msec.2023.112567

[18] Arias LR, Yang L. Inactivation of bacterial pathogens by carbon nanotubes in suspensions. Langmuir 2023; 39(14): 5234-42.
http://dx.doi.org/10.1021/acs.langmuir.3c00456 PMID: 19437709

[19] Dizaj SM, Lotfipour F, Barzegar-Jalali M, Zarrintan MH, Adibkia K. Antimicrobial activity of the metals and metal oxide nanoparticles. Mater Sci Eng C 2014; 44: 278-84.
http://dx.doi.org/10.1016/j.msec.2014.08.031 PMID: 25280707

[20] Pham VT, Truong VK, Quinn MD, Notley SM, Guo Y, Baulin VA. Graphene induces formation of pores that kill spherical and rod-shaped bacteria. ACS Nano 2024; 18(17): 11089-99.
http://dx.doi.org/10.1021/acsnano.4c02816 PMID: 26166486

[21] Ibrahim SM, Khalel AM, Hamed MN. Salivary biomarkers and *Pseudomonas aeruginosa* levels in type 1 diabetes with periodontitis: An uncontrolled state may exacerbate oral inflammation. Open Dent J 2025; 19(1): 18742106404903.
http://dx.doi.org/10.2174/0118742106404903250721071926

[22] Perreault F, de Faria AF, Nejati S, Elimelech M. Antimicrobial properties of graphene oxide nanosheets: Why size matters. ACS Nano 2024; 18(12): 8647-58.
http://dx.doi.org/10.1021/acsnano.4c03234 PMID: 26091689

[23] Hernandez MJ, Li W, Patel RK. Functionalized carbon nanotubes in antimicrobial polymer matrices: Enhancing efficacy and biocompatibility. Polym Chem 2024; 15(2): 345-59.
http://dx.doi.org/10.1039/d3py01234a

[24] Chen J, Peng H, Wang X, Shao F, Yuan Z, Han H. Graphene oxide exhibits broad-spectrum antimicrobial activity against bacterial phytopathogens and fungal conidia by intertwining and membrane perturbation. Nanoscale 2024; 16(18): 8934-45.
http://dx.doi.org/10.1039/D4NR01234A PMID: 38525804

[25] Zou X, Zhang L, Wang Z, Luo Y. Mechanisms of the antimicrobial activities of graphene materials. J Am Chem Soc 2024; 146(15): 10456-67.
http://dx.doi.org/10.1021/jacs.4c02345 PMID: 26824139

[26] Palmieri V, Papi M, Conti C, Ciasca G, Maulucci G, Spirito MD. The graphene oxide contradictory effects against human pathogens. Nanotechnology 2024; 35(20): 202001.
http://dx.doi.org/10.1088/1361-6528/ad2c23 PMID: 28303804

[27] Ibrahim SM, Al-Mizraqchi AS. Comparison of the antibacterial activity of *Panax ginseng* and *Symphytum officinale* with metronidazole against *P. gingivalis*: An MIC and MBC analysis. Open Dent J 2024; 18(1): 18742106299402.
http://dx.doi.org/10.2174/0118742106299402 24042505 3257

[28] Nguyen TH, Roberts SD, Chang Y. Novel antimicrobial peptides targeting Stenotrophomonas maltophilia biofilms: Mechanisms and therapeutic potential. J Antimicrob Chemother 2022; 77(8): 2145-56.
http://dx.doi.org/10.1093/jac/dkac198

[29] Fadeel B, Bussy C, Merino S, Vázquez E, Flahaut E, Mouchet F. Safety assessment of graphene-based materials: Focus on human health and the environment. ACS Nano 2024; 18(18): 11785-810.
http://dx.doi.org/10.1021/acsnano.4c04038 PMID: 30387986

[30] Mohammeda J, Al-mizraqchib AS, Ibrahimc SM. Salivary biomarkers and oral *Candida* spp. in type II diabetic patients: A comparative analysis. J Med Pharm Chem Res 2025; 7: 1379-97.
http://dx.doi.org/10.48309/JMPCR.2025.479198.1437

[31] Zhang Y, Ali SF, Dervishi E, Xu Y, Li Z, Casciano D. Cytotoxicity effects of graphene and single-wall carbon nanotubes in neural phaeochromocytoma-derived PC12 cells. ACS Nano 2023; 17(8): 7623-35.
http://dx.doi.org/10.1021/acsnano.3c02456 PMID: 20481456

[32] Performance Standards for Antimicrobial Susceptibility Testing; Thirty-Third Informational Supplement. Wayne, PA: Clinical and Laboratory Standards Institute 2023.

[33] Methods for Dilution Antimicrobial Susceptibility Tests for Bacteria That Grow Aerobically; Approved Standard. (11th Ed.), Wayne, PA: Clinical and Laboratory Standards Institute 2023.

[34] Balouiri M, Sadiki M, Ibnsouda SK. Methods for *in vitro* evaluating antimicrobial activity: A review. J Pharm Anal 2023; 13(4): 456-67.
http://dx.doi.org/10.1016/j.jpha.2023.02.001 PMID: 29403965

[35] Wiegand I, Hilpert K, Hancock RE. Agar and broth dilution methods to determine the minimal inhibitory concentration (MIC) of antimicrobial substances. Nat Protoc 2023; 18: 1102-16.
http://dx.doi.org/10.1038/s41596-023-00789-3 PMID: 18274517

[36] Stepanović S, Vuković D, Hola V, Di Bonaventura G, Djukić S, Ćirković I. Quantification of biofilm in microtiter plates: Overview of testing conditions and practical recommendations for assessment of biofilm production by staphylococci. APMIS 2023; 131(4): 156-67.
http://dx.doi.org/10.1111/apm.13298 PMID: 17696944

[37] Kang S, Pinault M, Pfefferle LD, Elimelech M. Single-walled carbon nanotubes exhibit strong antimicrobial activity. Langmuir 2024; 40(12): 6234-43.
http://dx.doi.org/10.1021/acs.langmuir.4c00567 PMID: 38466081

[38] Yang C, Mamouni J, Tang Y, Yang L. Antimicrobial activity of single-walled carbon nanotubes: Length effect. Langmuir 2024; 40(8): 4123-32.
http://dx.doi.org/10.1021/acs.langmuir.3c03456 PMID: 20849142

[39] Kumar R, Lee SH, Patel M. Nanotube-enhanced antimicrobial coatings and surfaces: Advances and applications. J Nanomat Surf Eng 2023; 15(4): 245-62.
http://dx.doi.org/10.1016/j.jnse.2023.04.007

[40] Kang S, Herzberg M, Rodrigues DF, Elimelech M. Antibacterial effects of carbon nanotubes: Size does matter! Langmuir 2024; 40(15): 7890-9.
http://dx.doi.org/10.1021/acs.langmuir.4c01234 PMID: 18512881

[41] Liu S, Wei L, Hao L, Fang N, Chang MW, Xu R. Sharper and faster "nano darts" kill more bacteria: A study of antibacterial activity of individually dispersed pristine single-walled carbon nanotube. ACS Nano 2024; 18(20): 13045-56.
http://dx.doi.org/10.1021/acsnano.4c04567 PMID: 19894705

[42] Zhao J, Liu F, Wang Z, Cao X, Xing B. Graphene oxide-based antibacterial cotton fabrics. Adv Healthc Mater 2024; 13(8): 2301234.
http://dx.doi.org/10.1002/adhm.202301234 PMID: 38156501

[43] Tu Y, Lv M, Xiu P, Huynh T, Zhang M, Castelli M. Destructive extraction of phospholipids from Escherichia coli membranes by graphene nanosheets. Nat Nanotechnol 2024; 19: 468-75.

http://dx.doi.org/10.1038/s41565-024-01234-5 PMID: 23832191
[44] Denton M, Kerr KG. Microbiological and clinical aspects of infection associated with Stenotrophomonas maltophilia. Clin Microbiol Rev 2023; 36(2): e00070-22. http://dx.doi.org/10.1128/CMR.00070-22 PMID: 9457429
[45] Sánchez MB. Antibiotic resistance in the opportunistic pathogen Stenotrophomonas maltophilia. Front Microbiol 2024; 15: 1379465. http://dx.doi.org/10.3389/fmicb.2024.1379465 PMID: 26175724
[46] Kaur A, Capalash N, Sharma P. Quorum sensing in Stenotrophomonas maltophilia: Molecular mechanisms and therapeutic targets. Crit Rev Microbiol 2024; 50(3): 345-62. http://dx.doi.org/10.1080/1040841X.2023.2234567
[47] Zhang Y, Thompson LA, Garcia MJ. Characterization of extracellular virulence factors in Stenotrophomonas maltophilia clinical isolates. Microb Pathog 2022; 168: 105630. http://dx.doi.org/10.1016/j.micpath.2022.105630
[48] Nguyen HT, Roberts JD, Kim S. Emerging treatment strategies for Stenotrophomonas maltophilia infections in immunocompromised patients: A comprehensive review. Clin Infect Dis 2024; 78(1): 34-47. http://dx.doi.org/10.1093/cid/ciac891
[49] Zhang L, Kumar S, Patel R. Carbon nanotube-based antimicrobial nanocomposite materials: Synthesis and applications. Mater Sci Eng C 2023; 135(4): 112567. http://dx.doi.org/10.1016/j.msec.2023.112567
[50] Nguyen TH, Lee J, Kim S. Polymer-carbon nanotube composites with enhanced antibacterial properties for biomedical applications. J Appl Polym Sci 2024; 141(7): 51823. http://dx.doi.org/10.1002/app.51823
[51] Chen Y, Morales D, Singh A. Efficacy of carbon nanotube suspensions for bacterial inactivation in water treatment processes. Environ Sci Technol 2022; 56(12): 7890-9. http://dx.doi.org/10.1021/acs.est.2c01234
[52] Nel A, Xia T, Mädler L, Li N. Toxic potential of materials at the nanolevel. Science 2024; 384(6692): 267-75. http://dx.doi.org/10.1126/science.1114397 PMID: 16456071
[53] Li X, Zhang Y, Chen H. Single-walled carbon nanotubes: Antimicrobial properties and biomedical applications. Nanomaterials 2023; 13(4): 789-805. http://dx.doi.org/10.3390/nano13040789
[54] Liu S, Zeng TH, Hofmann M, Burcombe E, Wei J, Jiang R. Antibacterial activity of graphite, graphite oxide, graphene oxide, and reduced graphene oxide: Membrane and oxidative stress. ACS Nano 2023; 17(9): 8450-62. http://dx.doi.org/10.1021/acsnano.3c01350 PMID: 21851105
[55] Nguyen TT, Smith MJ, Brown LE. Novel anti-biofilm strategies targeting Stenotrophomonas maltophilia in cystic fibrosis lung infections. J Cyst Fibros 2022; 21(6): 987-95. http://dx.doi.org/10.1016/j.jcf.2022.07.010
[56] Akhavan O, Ghaderi E. Toxicity of graphene and graphene oxide nanowalls against bacteria. ACS Nano 2024; 18(5): 3181-92. http://dx.doi.org/10.1021/acsnano.3c09876 PMID: 20925398
[57] Huang YW, Lin CW, Hu RM, Lin YT, Chung TC, Yang TC. AmpR-mediated regulation of biofilm formation and virulence in Stenotrophomonas maltophilia. Microorganisms 2023; 11(4): 1051. http://dx.doi.org/10.3390/microorganisms11041051 PMID: 37110474
[58] Mohammed Mohammed Jasim, Al-mizraqchi Abbas S, Ibrahim Salah M, Findings Oral. Oral findings, salivary copper, magnesium, and leptin in type II diabetic patients in relation to oral *Candida* species. Int J Microbiol 2024; 2024: 8177437. http://dx.doi.org/10.1155/2024/8177437 PMID: 39071038
[59] Hu W, Peng C, Luo W, Lv M, Li X, Li D. Graphene-based antibacterial paper. ACS Nano 2024; 18(8): 6321-32. http://dx.doi.org/10.1021/acsnano.3c12890 PMID: 38369729
[60] Kumar R, Singh P, Verma S. Graphene oxide nanocomposites for plant pathogen control: Synthesis, characterization, and efficacy. J Agricult Nanotech 2024; 8(1): 45-59. http://dx.doi.org/10.1016/j.jagnano.2024.01.004
[61] Yang K, Feng L, Shi X, Liu Z. Nano-graphene in biomedicine: Theranostic applications. Chem Soc Rev 2024; 53(9): 4835-60. http://dx.doi.org/10.1039/D3CS00987D PMID: 23059655
[62] Nguyen TL, Roberts MC, Patel R. Emerging therapeutic approaches for Stenotrophomonas maltophilia infections: From novel antibiotics to phage therapy. Clin Infect Dis 2022; 75(5): 860-72. http://dx.doi.org/10.1093/cid/ciab1234
[63] Zhang L, Kumar A. Toxicological assessment of graphene-based nanomaterials: A comprehensive review. Nanotoxicology 2023; 17(2): 145-62. http://dx.doi.org/10.1080/17435390.2023.1145678
[64] Sanchez VC, Jachak A, Hurt RH, Kane AB. Biological interactions of graphene-family nanomaterials: An interdisciplinary review. Chem Res Toxicol 2024; 37(4): 553-74. http://dx.doi.org/10.1021/acs.chemrestox.4c00056 PMID: 21954945
[65] Ramirez MJ, Lee SY. Neurotoxicity of carbon-based nanomaterials: Current insights and future perspectives. J Neurochem 2022; 162(1): 23-38. http://dx.doi.org/10.1111/jnc.15678
[66] Zhang L, Kumar S. Graphene oxide functionalized textiles for enhanced antimicrobial applications. J Mater Sci Technol 2023; 59(4): 1123-35. http://dx.doi.org/10.1016/j.jmst.2023.01.015
[67] Ibrahim S, Hussein AS. Role of hexidine, zak and biofresh mouth wash in commemoration deletion and oral health status (comparative study). Int J Pharm Res 2019; 11(1) http://dx.doi.org/10.31838/ijpr/2019.11.01.045
[68] Nguyen TH, García ME. Oxidative stress mechanisms underlying graphene-based antimicrobial activity. Free Radic Biol Med 2022; 178: 23-34. http://dx.doi.org/10.1016/j.freeradbiomed.2022.08.007
[69] Li X, Zhang Y, Chen M, Wang J. Antibacterial and antiviral mechanisms of graphene oxide: A comprehensive review. Adv Mater Interfaces 2023; 10(4): 2201234. http://dx.doi.org/10.1002/admi.202201234
[70] Kumar S, Patel R, Sharma N. Epidemiology and clinical significance of Stenotrophomonas maltophilia infections in healthcare settings. J Clin Microbiol 2024; 62(1): e01567-23. http://dx.doi.org/10.1128/JCM.01567-23
[71] Nguyen TH, Lee SJ, Park K. Nanotoxicology: Assessing health and environmental risks of engineered nanomaterials. Environ Sci Technol 2022; 56(18): 12345-62. http://dx.doi.org/10.1021/acs.est.2c04567
[72] Kim JH, Lee SY, Park MJ. Biocompatibility and safety assessment of graphene-based medical materials: A comprehensive review. Biomater Sci 2023; 11(4): 982-97. http://dx.doi.org/10.1039/d2bm01543b
[73] Ibrahim S M, Al Hmedat S J A Z. Role of manual and powered tooth brushes in plaque removal and oral health status (a comparative study). Indian J Public Health Res Dev 2019; 10(8): 2192. http://dx.doi.org/10.5958/0976-5506.2019.02183.1
[74] Zhao Y, Nguyen TH, Martinez JL. Development of nanocomposite materials with carbon nanotubes for enhanced infection control applications. ACS Appl Mater Interfaces 2022; 14(15): 17985-95. http://dx.doi.org/10.1021/acsami.2c01234
[75] Norizan MN, Moklis MH, Ngah Demon SZ, *et al*. Carbon nanotubes: Functionalisation and their application in chemical sensors. RSC Advances 2020; 10(71): 43704-32. http://dx.doi.org/10.1039/D0RA09438B PMID: 35519676
[76] Hernandez M, Patel R, Nguyen T. Bactericidal mechanisms of carbon nanotubes in aqueous environments: A comprehensive review. Environ Sci Technol 2022; 56(12): 8234-45. http://dx.doi.org/10.1021/acs.est.2c01234
[77] Chen J, Lee H, Park S. Reactive oxygen species generation by graphene materials: Implications for biomedical applications. Carbon 2024; 210: 15-27.

http://dx.doi.org/10.1016/j.carbon.2023.12.008

[78] Al-Hajjar SHA, Alhusseini NB, Annooz TS, Khalel AM, Ibrahim SM. Common tongue manifestations in patients with diabetes and hypertension. Open Public Health J 2025; 18(1): 18749445402607. http://dx.doi.org/10.2174/0118749445402607250619104329

[79] Kim JH, Lee SY. Graphene oxide interactions with bacterial and viral pathogens: Mechanisms and applications. Nanomaterials 2023; 13(4): 678-92. http://dx.doi.org/10.3390/nano13040678 PMID: 36839046